Pergamon

Bioorganic & Medicinal Chemistry 10 (2002) 41–46

BIOORGANIC & MEDICINAL CHEMISTRY

An Oxyanion-Hole Selective Serine Protease Inhibitor in Complex with Trypsin

Jian Cui,[a,b] Fatima Marankan,[a] Wentao Fu,[a] David Crich,[b] Andrew Mesecar[a] and Michael E. Johnson[a,*]

[a]*Center for Pharmaceutical Biotechnology, College of Pharmacy, University of Illinois at Chicago, 900 S. Ashland Avenue, M/C 870, Chicago, IL 60607-7173, USA*

[b]*Department of Chemistry, University of Illinois at Chicago, 845 West Taylor Street, Chicago, IL 60607-7061, USA*

Received 19 April 2001; accepted 29 June 2001

Abstract—*p*-amidinophenylmethylphosphinic acid (**AMPA**) was designed, synthesized and crystallized in complex with trypsin to study interactions with the oxyanion hole at the S1 site. In comparison to benzamidine, **AMPA** shows improved activity, which the crystal structure demonstrates to result from hydrogen bonds between the negatively charged phosphinic acid group and the catalytic residues at the oxyanion hole.

Introduction

Thrombin, a serine protease of the trypsin family, plays a central role in thrombosis and hemostasis.[1] As the final enzyme controlling the blood coagulation cascade, it has been the target of extensive research into the development of new anticoagulant agents.[2–5] Similarly, factor Xa, the penultimate enzyme in the coagulation cascade, has received increasing attention in the development of new anticoagulant agents.[3,6–9] The enzymes of the blood coagulation cascade, including thrombin, factor Xa and factor VIIa are known to have specificity pockets (S1 subsites) very similar to those of other serine proteases such as trypsin and plasmin. The Asp189 residue at the bottom of the pocket binds ionically with arginyl or benzamidinium ionic groups. In our prior development of thrombin inhibitors with *N*-(2-naphthylsulphonyl-glycyl)-D-*p*-amidinophenylalanyl-piperidine (NAPAP)[10] as a template, we used α-aminophosphinates as a key building block in a dipeptide mimetic design.[11] However, detailed computational analysis of the bound conformational model suggests that the phosphinate is not well positioned into the oxyanion hole, and that structural specificity could be substantially enhanced by positioning the phosphinate closer to the oxyanion hole (Fig. 1).

We report here a study at the S1 site using *p*-amidinophenylphosphinic acid as an initial 'building block' for the development of higher affinity serine protease inhibitors using phosphinic acid as a key moiety. The use of phosphinic acid as a tetrahedral state analogue in inhibitors of a wide variety of proteases has been recently reviewed, with the literature indicating that it provides a very effective transition state analogue in a structurally and chemically diverse range of inhibitors.[12]

Design of an S1 site-selective inhibitor

In selecting phosphinic acid as a key building block, our hypothesis is that the oxyanion hole at the entrance to the serine protease S1 site is important for the binding of substrate and stabilization of the tetrahedral intermediate. In order to study the interactions at the S1 site, *p*-amidinophenylmethylphosphinic acid (**AMPA**) was designed and synthesized (Scheme 1), with the two carbon linker between the benzyl and phosphinic acid of our prior inhibitor (Fig. 1) removed to better position the phosphinic acid with respect to the oxyanion hole.

At the oxyanion hole, several main chain residues can act as hydrogen bond donors to form hydrogen bonds with carbonyl groups or negative charges from substrates or inhibitors. These hydrogen bonds could form between the negatively charged phosphinic acid and the hydrogen bond donors at the oxyanion hole, and thus contribute to binding and improvement in activity.

*Corresponding author. Tel.: +1-312-996-9114; fax: +1-312-413-9303; e-mail: mjohnson@uic.edu

0968-0896/02/$ - see front matter
PII: S0968-0896(01)00259-0

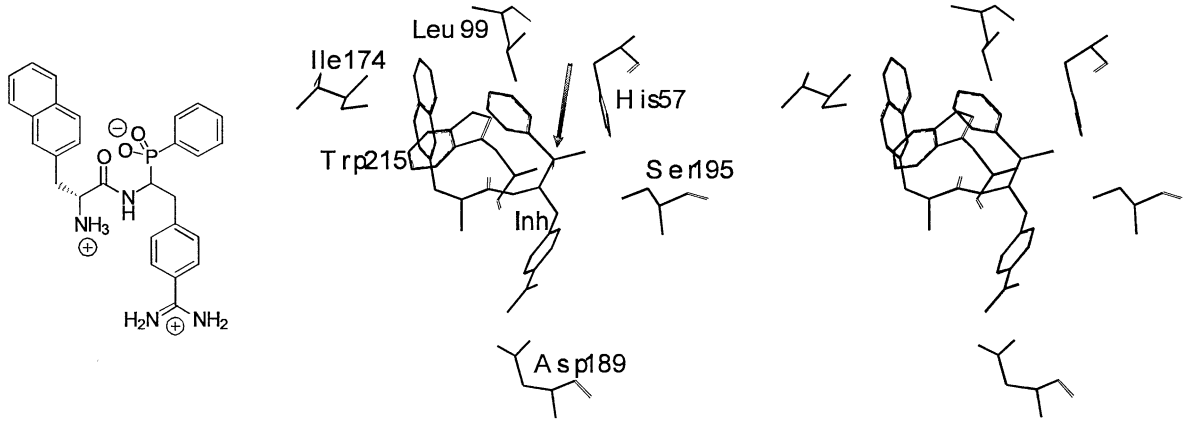

Figure 1. Thrombin inhibitor ($IC_{50} = 0.6$ M) from our prior work,[11] using α-aminophosphinate as the key building block. Schematic structure shown at the left; modeled structure in the thrombin catalytic site shown in relaxed stereo to the right, with arrow pointing toward the center of the phosphinate group.

Chemistry

The synthesis of **AMPA** is outlined in Scheme 1. Copper bromide catalyzed reaction of 4-cyanobenzenediazonium tetrafluoroborate[13] with PCl_3 and then magnesium in ethyl acetate gave the phosphorus dichloride **1**.[13] In situ treatment with methanol in pyridine then afforded the phosphonous acid dimethyl ester **2**, which, on heating to reflux with neat methyl iodide,[14,15] gave the Arbuzov product (**3**). This nitrile was converted to the amidine **6** by a three step protocol involving reaction with diethyl dithiophosphoric acid to give thioamide **4**, alkylation to afford the thioimidate **5** and exposure to ammonium acetate in acetonitrile. Finally, the phosphinate ester was hydrolyzed by treatment with 5% aqueous sodium hydroxide, and **AMPA** was isolated by reverse phase HPLC.

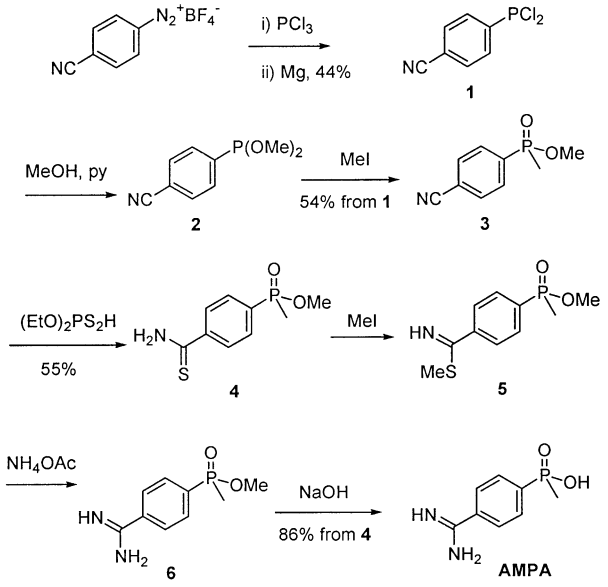

Scheme 1. Synthesis of *p*-amidinophenyl-methyl-phosphinic acid (**AMPA**).

Results and Discussion

AMPA was evaluated for its potency in serine protease inhibition using the chromogenic substrates *N*-*p*-tosyl-Gly-Pro-Arg-*p*NA (thrombin, trypsin), MeO-CO-D-CHG-Gly-Arg-*p*NA (factor Xa) and D-Val-Leu-Lys-*p*NA (plasmin); the released nitrophenol was monitored at 405 nm. The in vitro inhibitory assay results are shown in Table 1.

AMPA was designed and synthesized as an S1 site probe; the S1 recognition site exhibits little structural variation among the various serine proteases. Thus, the lack of significant selectivity among the various enzymes is expected. In comparison with benzamidine under the same assay conditions, *p*-amidinophenylmethylphosphinic acid (**AMPA**) shows varied, but consistent improvement in activity (5 times for factor Xa, 12 times for thrombin, 6 times for trypsin and 3 times for plasmin).

The X-ray crystallographic data collection, processing and refinement statistics for the structure of bovine trypsin complexed with **AMPA** are summarized in Table 2. The structure was solved to 1.75 Å resolution and to a final R factor of 18.2%. The electron density for **AMPA** in the active site of the complex is shown in Figure 2 along with a detailed view of the interactions between **AMPA** and the enzyme. The electron density is well ordered and unambiguous for **AMPA** and sur-

Table 1. In vitro inhibitory activities of *p*-amidinophenylmethylphosphinic acid (**AMPA**)

	K_i (μM)[a]			
	Factor Xa	Thrombin	Trypsin	Plasmin
AMPA	106	44	25	79
Benzamidine	490	550	150	250

[a]Assays were performed at 37 °C in a semimicrocuvette. Reaction rates were determined by measuring the rate of the absorbance change at 405 nm in a Beckman 2400 spectrophotometer or a Shimadzu UV-2401PC UV–vis recording spectrophotometer.

rounding water molecules. The position of the methyl group of phosphinic acid was modeled into the electron density based on the fact that the electron density associated with this atom was more extended than the electron density associated with the phosphinic oxygen atoms (Fig. 2B). The approximate bond lengths for the P−CH_3 and the P=O bonds are ~1.82 and ~1.52 Å based upon model compounds (reference codes: SOJKIL, HEQYEH, NALWOM, SOSKEH, JIBVEV) in the Cambridge Structural Database[16–18] and our final refined model.

The phosphinic acid methyl group points directly toward the S4 site as predicted from computer modeling (Fig. 2C). However, the position of the phosphinic acid moiety in the oxyanion hole occupies a position slightly different than that predicted from computer modeling (not shown). The predicted position placed the phosphinic acid group directly in the oxyanion hole and within hydrogen bond distance of the backbone amides of Glycine 193 and Serine 195, similar to the B_{LIG} oxyanion site as defined by Presnel et al.[19]

Table 2. X-ray crystallographic data collection, processing and refinement statistics for bovine trypsin complexed with *p*-amidinophenylmethylphosphinic acid (**AMPA**)

Crystal conditions	Room temperature—298 °K
X-ray source	RU-200 and Raxis IIC
Resolution (Å)	1.75
Crystal to detector distance (mm)	80
Exposure time (min/degree)	8
Rotations (*n*, degree)	100 @ 1°
Overall data statistics [outer shell]	
Data range (Å)	50–1.75 [1.78–1.75]
Total measured reflections (*n*)	125,665
Rejected reflections (*n*)	1068
Unique possible reflections (*n*)	22,550
Unique measured reflections (*n*)	20,953
Percent completeness (%)	92.9 [64.6]
Average redundancy	6
Average I/σI	22.6 [8.1]
R_{merge} (%) overall	7.8 [16.1]
Space group	$P2_12_12_1$
Cell dimensions (Å)	a = 54.87, b = 58.44, c = 67.52
Mosaic spread (°)	0.25
Molecules per asymetric unit (*n*)	1
Refinement statistics [outer shell]	
Resolution range	50.0–1.75 [1.83–1.75]
Reflections	
Included ($F > 2\sigma$)	19,163
Excluded for R_{free} (5%)	981
R_{cryst} (%)	18.2 [23.9]
R_{free} (%)	23.0 [29.0]
Molecules in final model (*n*) and B-factors (Å^2)	
Protein residues	229 [buried = 10.5]
AMPA	1 [23.7]
Ca^{2+}	1 [11.2]
H_2O	93
Ramachandaran plot	
core (%)	85.1
allowed (%)	14.9
generous (%)	0
disallowed (%)	0

In contrast, the X-ray crystal structure of the trypsin–**AMPA** complex shows that oxygen-2 (O_2) of the phosphinic acid moiety forms direct hydrogen bonds with the N_ε nitrogen of Histidine-57 (2.69 Å) and with the sidechain oxygen of Serine-195 (2.42 Å). In addition, the O_1 and O_2 oxygens of the phosphinic acid group both form hydrogen bonds with a single water molecule (O_1 and O_2 distances to water oxygen of 3.14 and 2.90 Å, respectively) that is anchored by a single hydrogen bond to the backbone amide of Glycine 193 (3.09 Å) (Fig. 2C). This water nearly occupies the B_{LIG} oxyanion site by overlapping the position of the sulfate ion (SO_4^{2-}) in bovine trypsin complexed with the benzamidine derivatives 1-(4-amidinophenyl)-3-(4-chlorophenyl)urea (ACPU) and 1-(4-amidinophenyl)-3-(4-phenyoxyphenyl)-urea (APPU) and the SO_4^{2-} ion.[19]

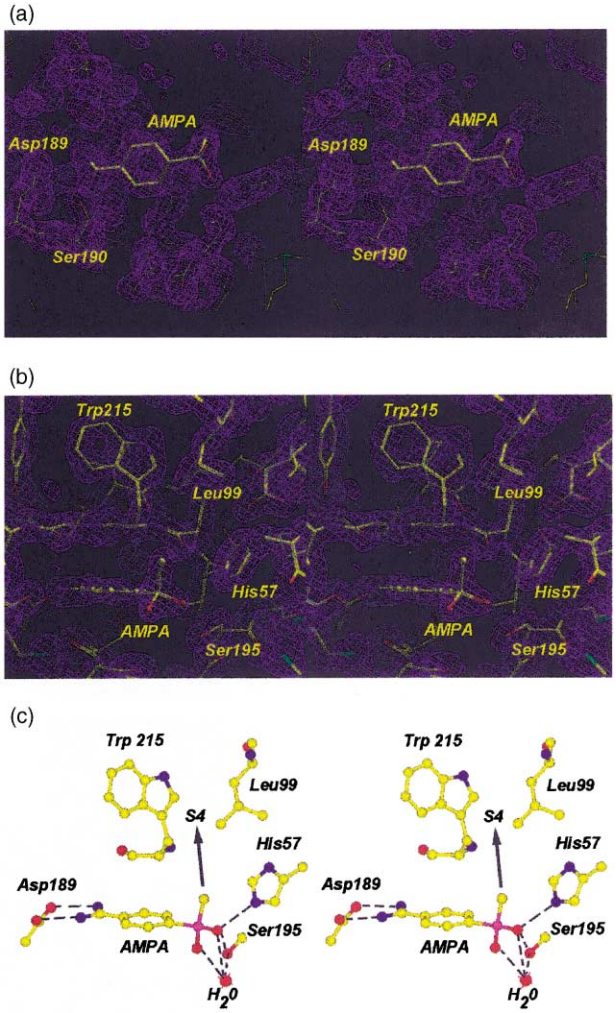

Figure 2. Relaxed stereoviews of the active site of bovine trypsin complexed with amidinophenylmethylphosphinic acid (**AMPA**). Panel (**A**) is the final (2Fo-Fc)α_{calc} electron density map contoured at 1.0 σ. The orientation of **AMPA** was chosen to highlight the quality of the electron density of the inhibitor. Panel (**B**) is also the final (2Fo-Fc)α_{calc} electron density map contoured at 1.0 σ. Here, the orientation of **AMPA** was chosen to illustrate the elongated density in the region of the phoshinic acid methyl group and to show the position of the methyl group relative to the S4 pocket. Panel (**C**) shows the hydrogen bonding interactions between **AMPA** and the protein and water molecule in the oxyanion hole.

The position of the oxygen atoms of the phosphinic acid group in the X-ray structure indicates that this group occupies a unique oxyanion hole position in the trypsin active site compared to those of oxyanion hole sites (A_{LIG}, B_{LIG}, A_{TET}, and B_{TET}) of serine proteases in general.[19] The hydrogen bond distances of the phosphinic oxygen atom O_2 to the ε-nitrogen of Histidine-57 and to the side chain oxygen of Serine-195 are comparable to those observed in the tetrahedral (A_{TET}) site of serine proteases ($N\varepsilon2_{His57}$–O distance 2.8 Å and $O\gamma_{Ser195}$–O distance of 2.3 Å). In addition, no hydrogen bonds exist between the phosphinic acid O_2 and the backbone amides of residues 193 to 195 are observed as predicted by the A_{TET} position. However, the defined bond angles for the A_{TET} site ($C\varepsilon1_{His57}$–$N\varepsilon2_{His57}$ of 137° and $C\beta1_{Ser195}$–$O\gamma_{Ser195}$ of 109°) are inconsistent with the observed angles of ($C\varepsilon1_{His57}$–$N\varepsilon2_{His57}$ of 117° and $C\beta1_{Ser195}$–$O\gamma_{Ser195}$ of 101°) in the X-ray structure.

The positioning of the methyl group on the phosphinic acid moiety suggests that **AMPA** will indeed be a useful template for the design of novel serine protease inhibitors. Moreover, the unique binding mode of **AMPA** uncovered by the crystal structure suggests that some flexibility in positioning of oxygen atoms within the oxyanion hole exists. Such flexibility could be useful in strengthening the interaction of the template with the oxyanion hole by additional substitution. The observation that a water molecule bridges two of the three hydrogen bonds between the phosphinic acid group and fXa may partly explain the relatively modest K_i decrease from benzamidine to AMPA, and suggests that further structural alterations may be useful.

Experimental

General experimental

^1H, ^{13}C and ^{31}P NMR spectra were recorded as $CDCl_3$ solutions at 300, 75.5 and 121.5 MHz, respectively, unless otherwise mentioned. All solvents were dried and distilled by standard methods. Microanalyses were carried out at Midwest Microlabs, Indianapolis, IN.

***p*-Cyanophenyldichlorphosphine (1).** A 500-mL, three-necked, round-bottomed flask equipped with a thermometer and an efficient reflux condenser was charged with 4-cyanobenzenediazonium tetrafluoroborate[13] (4.34 g, 20 mmol), CuBr (170 mg, 1.2 mmol), and ethyl acetate (20 mL). Phosphorous trichloride (2 mL, 23 mmol) was added dropwise at room temperature over 15 min. After stirring for 30 min., the mixture was cautiously warmed to 40 °C, a vigorous exothermic reaction occurred and large amount of gas was evolved (a large flask with an efficient condenser is suggested). The reaction mixture was stirred for 1 h at 45 °C before magnesium turnings (0.5 g, 20 mmol) were added piece by piece over 1 h while the internal temperature was maintained between 30 and 40 °C. After 2–3 h, all the magnesium had dissolved and the brown mixture turned to a red solution. This was concentrated and the residual semi-solid mass was extracted with 1:1 (v/v) benzene/heptane (3×20 mL). The combined extracts were freed of solvent and the residual liquid then distilled under vacuum. Dichloride **1**[13] (1.81 g, 44%) was collected at 120 °C at 2 mmHg as a colorless liquid. ^1H NMR δ 8.00 (2H, t, $J=7.8$ Hz), 7.80 (2 H, d, $J=7.9$ Hz); ^{31}P NMR δ 155.4.

Methyl *p*-Cyanophenylmethylphosphinate (3). A mixture of **1** (3.41 g, 16.7 mmol) and dry pyridine (2.8 mL) in hexanes (9 mL) was cooled in an ice-water bath, and a solution of methanol (1.4 mL) and hexanes (0.5 mL) was added dropwise under argon. After stirring at 0 °C for 1 h, the white precipitate was removed by filtration under a stream of dry argon. The filtrate was concentrated under reduced pressure to give dimethyl 4-cyanophenylphosphonite (**2**) as a yellow oil, which was not further purified. Several drops of the crude phosphonite and a few drops of methyl iodide were added to a 25 mL flask equipped with a reflux condenser and heated to 100 °C. The remaining phosphonite and further methyl iodide were then added periodically to ensure a continuous reaction. After 1 h at 100 °C, the reaction mixture was cooled to room temperature and stirred overnight to give a yellow semi-solid, which was purified by column chromatography to give **3** (1.76 g, 54% from **1**) as a colorless liquid. ^1H NMR (Methanol-d_4) δ 8.01–7.88 (4 H, m), 3.65 (3 H, d, $J=11.4$ Hz), 1.76 (3 H, d, $J=14.8$ Hz); ^{31}P NMR (Methanol-d_4) δ 49.7; ESIMS m/z 196.1 $(M+1)^+$. Anal. calcd for $C_9H_{10}NO_2P.1/4H_2O$: C, 54.15; H, 5.30; N, 7.02. Found: C, 54.44; H, 5.26; N, 6.98.

Methyl *p*-Thiocarbamoylphenylmethylphosphinate (4). A mixture of **3** (0.39 g, 2 mmol) and diethyl dithiophosphate (2 mL) with several drops of water was stirred at room temperature for two days, then diluted with ethyl acetate and washed with large amount of saturated aqueous $NaHCO_3$. The organic phase was dried (Na_2SO_4), concentrated and purified by column chromatography to give **4** (0.25 g, 55%) as a yellow semi-solid that was immediately used in the next step. ^1H NMR δ 7.95 (2 H, dd, $J=8.1$ Hz, 2.5 Hz), 7.77 (2 H, dd, $J=11.4$ Hz, 8.2 Hz), 7.74 (2H, br s), 3.61 (3H, d, $J=11.4$ Hz), 1.68 (3H, d, $J=14.7$ Hz); ^{31}P NMR δ 44.2; ESIMS m/z 230.1 $(M+1)^+$.

***p*-Amidinophenylmethylphosphinic Acid (AMPA).** A solution of **4** (0.16 g) in acetone (3 mL) was treated with methyl iodide (1 mL) and heated to reflux for 1.5 h, then concentrated to give crude **5** as a brown solid. This solid was suspended in acetonitrile, treated with ammonium acetate (65 mg) at 0 °C, and stirred overnight. After removing the solvent, crude **6** was collected as a sticky yellow solid. This was treated with 5% aqueous NaOH at room temperature for 1 h before the aqueous phase was washed with ethyl acetate and acidified with 2 N HCl. The resulting mixture was diluted with water to a final volume of 10 mL. Purification of 20×50 μL aliquots of the solution by semi-preparative HPLC (Beckman Ultrasphere C-18 column) using a 15–20% gradient of solvent A (0.1% TFA in acetonitrile) in solvent B (0.1% TFA in water) yielded **AMPA** (19 mg, 86% from **4**), which was collected as a brown solid (mp >280 °C dec) after concentration under vacuum. ^1H

NMR (Methanol-d_4) δ 8.03 (2H, dd, $J=11.6$ Hz, 8.4 Hz), 7.93 (2H, dd, $J=8.3$ Hz, 2.7 Hz), 1.69 (3H, d, $J=14.8$ Hz); ^{13}C NMR (Methanol-d_4) δ 167.8, 141.7, 140.0, 132.3 (d, $J=10.6$ Hz), 129.0 (d, $J=12.7$ Hz), 16.1 (d, $J=100.8$ Hz); ^{31}P NMR (Methanol-d_4) δ 42.3; ESIMS m/z 199.2 $(M+1)^+$. Anal. calcd for $C_8H_{11}N_2O_2P\cdot 1CF_3COOH$: C, 38.47; H, 3.87; N, 8.97. Found: C, 38.07; H, 3.88; N, 8.47.

Enzyme assays. Human fXa was obtained from American Diagnostica, Inc., Greenwich, CT. Human thrombin, bovine trypsin and human plasmin were from Sigma, St. Louis, MO. The activities of human fXa, human thrombin, bovine trypsin and human plasmin were monitored by rates of cleavage of peptide *p*-nitroanilide by the enzymes. The initial reaction rates were determined from the rate of change of absorbance at 405 nm using either a Beckman 2400 spectrophotometer or a Shimadzu UV-2401PC UV–vis recording spectrophotometer. Reactions were conducted at 37 °C in a semi-micro cuvette. Anti-fXa activities were measured using the chromogenic substrate MeO-CO-D-CHG-Gly-Arg-*p*NA (American Diagnostica, Inc.) and human fXa; assays were performed according to the manufacturers' protocols. Anti-thrombin and anti-trypsin activities were measured using the manufacturers' protocols (Sigma), using the chromogenic substrates *N*-*p*-tosyl-Gly-Pro-Arg-*p*NA (human thrombin) and *N*-*p*-tosyl-Gly-Pro-Arg-*p*NA (bovine trypsin). For the inhibition assays, AMPA was added in a 15 μL aliquot in a DMSO solution. The concentrations of substrates used in the inhibition assays were 20.1 μM (thrombin), 40.2 μM (trypsin) and 302 μM and 206 μM (plasmin). K_m and V_{max} values were determined from initial rates measured at varying substrate concentrations where the data was fit to the Michaelis–Menten equation using the program TableCurve 2D (v4.07, SPSS Scientific). Competitive inhibition was assumed, and initial rates for the inhibition assays were measured at different inhibitor concentrations. K_i values were calculated from a Dixon analysis[20] of the data using Origin 5.0 software (Microcal Software, Inc.).

Computer modeling. The starting geometry of the probe **AMPA** was optimized at the AM1 level of theory in the Gaussian98 suite of programs. AM1 charges were used for atomic charges. The optimized conformer was docked into the factor Xa active site using the Autodock program (version 3.0, Scripps Research Institute). The genetic Algorithm (GA) search method was used, with population size = 50, generations = 27,000, mutation rate = 0.02 and crossover rate = 0.80. Factor Xa crystal structures were obtained from the Protein Databank (accession codes: 1HCG, 1FAX).[21,22] Results were visualized using InsightII (MSI, Inc.) running on a Silicon Graphics O_2 workstation.

Trypsin crystallization and X-ray data collection. Bovine trypsin (Sigma) was co-crystallized with AMPA by a macroseeding procedure in a manner similar to that of Zhang et al.[23] Small rod-shaped crystals that formed were enlarged by macroseeding by placing the crystal in a pre-equilibrated drop with a slightly lower concentration of $(NH_4)_2SO_4$ (1.7 M) and 5 mM AMPA. After a few days of growth, enlarged crystals ($\sim 1\times 0.2\times 0.2$ mm) were obtained. A single crystal was mounted in a quartz capillary tube and X-ray diffraction data were collected at room temperature on an R-Axis IIc imaging plate using a Rigaku RU200 rotating anode X-ray source operating at 50 kV and 100 mA. The data were then processed and scaled with DENZO and SCALEPACK.[24] The resulting statistics are shown in Table 2.

Refinement. A single molecular replacement solution was found using the program EPMR (version 2.4)[25] and the coordinates of bovine trypsin complexed with (+/−)methyl 4-(aminoimino)phenyl-β-[3-inh(aminoimino)-phenyl]benzene pentanoate (PDB code 1AZ8).[26] Rigid-body refinement was followed by a single round of simulated annealing refinement using the slow-cool refinement protocol in X-PLOR[27] with 25 K steps and a starting temperature of 4000 K. Initial difference Fourier maps were calculated prior to any other refinements using the programs X-PLOR and CCP4.[28] Electron density maps were observed using the programs O[29] and SPOCK,[30] and all additional refinement protocols were performed using the program X-PLOR. An atomic model for **AMPA** was built using the Builder Module of InsightII (Molecular Simulations, Inc.). The model was then energy minimized using X-PLOR-2D and the appropriate topology and parameter files were generated using the same program.[31] After manually building **AMPA** and Ca^{2+} into the corresponding electron density, protein models were further refined using a series of iterations of positional and individual B-factor refinements with bulk solvent corrections until the R_{Free} values no longer decreased. Water molecules were added to peaks above 3σ. After all refinements, each structure was analyzed for geometric quality using PROCHECK,[32] WHATCHECK[33] and X-PLOR. Superpositions and RMS deviations in atomic positions were calculated using the program InsightII. The final refinement statistics are shown in Table 2.

Acknowledgements

We thank Dr. Debbie Mulhearn for a search of the Cambridge Structural Database for representative AMPA compounds and Dr. Zhao Lan Lin for the thrombin-inhibitor model shown in Figure 1. Supported in part by grants from the NIH and the UIC Campus Research Board. ADM is supported by a grant from the American Association of Colleges of Pharmacy, the Hans Vahlteich Endowment for faculty research, and the UIC/NIH Center for Dietary Botanical Supplements.

References and Notes

1. Becker, R. C.; Spencer, F. A. *J. Thromb. Thrombolysis* **1998**, *5*, 215.
2. Bursi, R.; Grootenhuis, P. D. *J. Comput. Aided Mol. Des.* **1999**, *13*, 221.
3. Fevig, J. M.; Wexler, R. R. *Annu. Rep. Med. Chem.* **1999**, *34*, 81.
4. Menear, K. *Curr. Med. Chem.* **1998**, *5*, 457.

5. Sanderson, P. E.; Naylor-Olsen, A. M. *Curr. Med. Chem.* **1998**, *5*, 289.
6. Nicolini, F. A.; Lee, P.; Malycky, J. L.; Lefkovits, J.; Kottke-Marchant, K.; Plow, E. F.; Topol, E. J. *Blood Coagul. Fibrinolysis* **1996**, *7*, 39.
7. Rai, R.; Sprengeler, P. A.; Elrod, K. C.; Young, W. B. *Curr. Med. Chem.* **2001**, *8*, 101.
8. Vacca, J. P. *Curr. Opin. Chem. Biol.* **2000**, *4*, 394.
9. Zhu, B. Y.; Scarborough, R. M. *Annu. Rep. Med. Chem.* **2000**, *35*, 83.
10. Brandstetter, H.; Turk, D.; Hoeffken, H. W.; Grosse, D.; Sturzebecher, J.; Martin, P. D.; Edwards, B. F.; Bode, W. *J. Mol. Biol.* **1992**, *226*, 1085.
11. Li, M.; Lin, Z.; Johnson, M. E. *Bioorg. Med. Chem. Lett.* **1999**, *9*, 1957.
12. Collinsova, M.; Jiracek, J. *Curr. Med. Chem.* **2000**, *7*, 629.
13. Quin, L. D.; Humphrey, J. S., Jr. *J. Am. Chem. Soc.* **1960**, *82*, 3795.
14. Harwood, H. J.; Grisley, D. W., Jr. *J. Am. Chem. Soc.* **1960**, *82*, 423.
15. Korpiun, O.; Lewis, R. A.; Chickos, J.; Mislow, K. *J. Amer. Chem. Soc.* **1968**, *90*, 4842.
16. Allen, F. H.; Kennard, O. *Chem. Des. Automation News* **1993**, *8*, 31.
17. Allen, F. H. *Trans. Am. Crystallogr. Assoc.* **2000**, *32*, 1.
18. Bruno, I. J.; Cole, J. C.; Lommerse, J. P.; Rowland, R. S.; Taylor, R.; Verdonk, M. L. *J. Comput. Aided Mol. Des.* **1997**, *11*, 525.
19. Presnell, S. R.; Patil, G. S.; Mura, C.; Jude, K. M.; Conley, J. M.; Bertrand, J. A.; Kam, C. M.; Powers, J. C.; Williams, L. D. *Biochemistry* **1998**, *37*, 17068.
20. Dixon, M. *Biochem. J.* **1953**, *55*, 170.
21. Padmanabhan, K.; Padmanabhan, K. P.; Tulinsky, A.; Park, C. H.; Bode, W.; Huber, R.; Blankenship, D. T.; Cardin, A. D.; Kisiel, W. *J. Mol. Biol.* **1993**, *232*, 947.
22. Brandstetter, H.; Kuhne, A.; Bode, W.; Huber, R.; von der, S. W.; Wirthensohn, K.; Engh, R. A. *J. Biol. Chem.* **1996**, *271*, 29988.
23. Krishnan, R.; Zhang, E.; Hakansson, K.; Arni, R. K.; Tulinsky, A.; Lim-Wilby, M. S.; Levy, O. E.; Semple, J. E.; Brunck, T. K. *Biochemistry* **1998**, *37*, 12094.
24. Otwinowski, Z.; Minor, W. *Methods Enzymol.* **1997**, *276*, 307.
25. Kissinger, C. R.; Gehlhaar, D. K.; Fogel, D. B. *Acta Crystallogr. D. Biol. Crystallogr.* **1999**, *55* (Pt 2), 484.
26. Maduskuie, T. P., Jr.; McNamara, K. J.; Ru, Y.; Knabb, R. M.; Stouten, P. F. *J. Med. Chem.* **1998**, *41*, 53.
27. Brünger, A. T. X-PLOR, version 3.5.1, a system for X-ray crystallography and NMR; Yale University Press: New Haven, CT, 1992.
28. Bailey, S. *Acta Crystallogr., Sect. D: Biol. Crystallogr.* **1994**, *D50*, 760.
29. Jones, T. A.; Zou, J. Y.; Cowan, S. W. *Kjeldgaard Acta Crystallogr. A* **1991**, *47* (Pt 2), 110.
30. Christopher, J. A. SPOCK: The Structural Properties Observation and Calculation Kit. 1997. College Station, TX, The Center for Macromolecular Design, Texas A&M University.
31. Kleywegt, G. J.; Jones, T. A. *Methods Enzymol.* **1997**, *277*, 208.
32. Laskowski, R. A.; MacArthur, M. W.; Moss, D. S.; Thornton, J. M. *J. Appl. Crystallogr.* **1993**, *26*, 283.
33. Hooft, R. W.; Vriend, G.; Sander, C.; Abola, E. E. *Nature* **1996**, *381*, 272.